V.V. ROMAKA,[1] V.A. ROMAKA,[2] YU.V. STADNYK,[3] L.P. ROMAKA,[3]
Y.O. PLEVACHUK,[3] A.M. HORYN,[3] V.Z. PASHKEVYCH,[2] P.I. HARANIUK[2]

[1] Leibniz Institute for Solid State and Materials Research (IFW) Dresden
  (Helmholtzstr. 20, 01069 Dresden, Germany; e-mail: v.romaka@ifw-dresden.de)
[2] Lviv Polytechnic National University
  (12, S. Bandera Str., Lviv 79013, Ukraine)
[3] Ivan Franko National University of Lviv
  (6, Kyryla and Mefodiya Str., Lviv 79005, Ukraine)

FEATURES OF THE GENERATION OF ENERGY STATES IN THE $Lu_{1-x}V_xNiSb$ SEMICONDUCTOR

A comprehensive study of the crystal and electronic structures, thermodynamic, kinetic, energy, and magnetic properties of the $Lu_{1-x}V_xNiSb$ semiconductor ($x = 0\div0.10$) has revealed the possibility for impurity V atoms to simultaneously occupy different crystallographic positions. At the same time, defects of the acceptor or donor nature are generated in the crystal structure of the $Lu_{1-x}V_xNiSb$ solid solution, and the corresponding energy states appear in the band gap ϵ_g. The concentration ratio of donor-acceptor states determines the position of the Fermi level ϵ_F and the mechanisms of electrical conductivity of $Lu_{1-x}V_xNiSb$. The results of the modeling of thermodynamic and transport properties of the semiconductor are consistent with experimental data. Understanding the mechanism of energy state generation in the semiconductor $Lu_{1-x}V_xNiSb$ allows the modeling and production of new thermoelectric materials with a high efficiency of converting the thermal energy into the electrical one.

K e y w o r d s: Fermi level, electronic structure, electrical resistivity, thermopower coefficient.

1. Introduction

Continuing the program of the finding of new thermoelectric materials, the structural, thermodynamic, magnetic, kinetic, and energy properties of the semiconductor solid solution $Lu_{1-x}V_xNiSb$, $x = 0\div0.10$, obtained by doping the p-LuNiSb semiconductor with V atoms through replacing the rare earth Lu atoms

in the crystallographic site $4a$, were investigated. The peculiarity of such doping is that V atoms, having a relatively small atomic radius ($r_V = 0.134$ nm) and the ability to be in different valence states, may show a variability in entering the structure of compounds and may occupy different crystallographic positions. This leads to the simultaneous generation of the defects of the acceptor, donor, or neutral nature in different ratios in the crystal structure, and the corresponding energy states appear in the band gap ϵ_g. In addition, the ability of V atoms to change the valence state can change the magnetic state of the material.

Solid solutions based on semiconductor half-Heusler phases (structure type of MgAgAs, space group $F\bar{4}3m$ [1]), in particular, TiNiSn, ZrNiSn, HfNiSn, TiCoSb, VFeSb, ZrCoSb, and RNiSb (R is a rare earth metal) are among the most studied thermo-
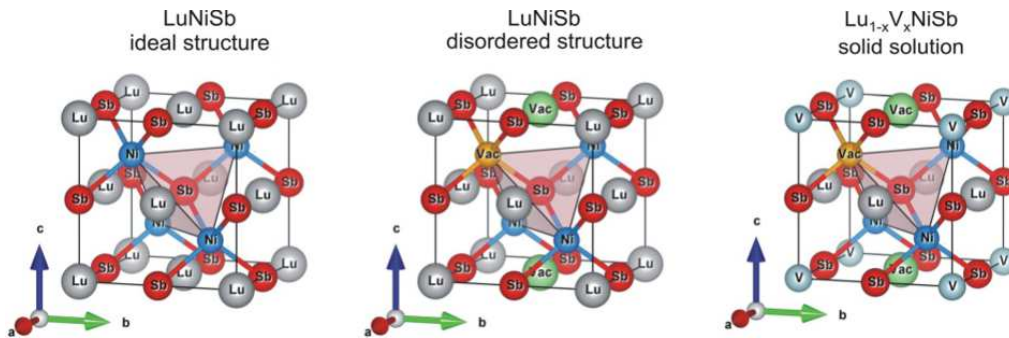
Fig. 1. Models of the crystal structure of LuNiSb and $Lu_{1-x}V_x$NiSb

electric materials, because they have a high efficiency of converting the thermal energy into the electrical one [2]. Previous studies of the RNiSb half-Heusler phases (R–Y, Gd–Lu) [3–6] revealed some disorder of the crystal structure, and the authors of work [7] established its nature. It was shown that, in the crystallographic positions $4a$ of R atoms and $4c$ of Ni atoms (Fig. 1), there are vacancies (Vac), which are structural defects of the acceptor nature and generate acceptor states ϵ_1^A in the band gap ϵ_g, while holes are the main carriers of electricity. This is indicated by the positive values of the thermopower coefficient $\alpha(T)$ [7].

In the studies of half-Heusler phases which contain V, in particular, in semiconductors $Zr_{1-x}V_x$NiSn [8], $Ti_{1-x}V_x$NiSn [9], $Ti_{1-x}V_x$CoSb [10], and $V_{1-x}Ti_x$FeSb [11], the mechanisms of simultaneous generation of structural defects of the acceptor and donor nature were revealed. Thus, thermodynamic calculations showed that, in $Zr_{1-x}V_x$NiSn, it is energetically favorable for V atoms to simultaneously partially occupy the $4c$ position of Ni atoms ($3d^8 4s^2$), which generates structural defects of the acceptor nature (V has fewer $3d$-electrons than Ni), as well as the $4a$ position of Zr atoms ($4d^2 5s^2$), generating defects of the donor nature (V has more d-electrons than Zr). In the $Zr_{1-x}V_x$NiSn band gap, energy states of the donor and acceptor nature appear simultaneously in different ratios. The results of kinetic and energy studies of $Zr_{1-x}V_x$NiSn coincided with the results of DFT calculations of the density of electronic states for the case where the total concentration of V atoms (x) is distributed between two positions: $4a$ of Zr atoms (y) and $4c$ of Ni atoms (z), and $x = y + z$. In this case, the formula of the solid solution is transformed into $(Zr_{1-y}V_y)(Ni_{1-z}V_z)$Sn [8].

At the same time, the introduction of atoms larger than V into the p-LuNiSb structure, in particular, Zr or Sc ($d^1 4s^2$) by substituting Lu atoms in the $4a$ position, did not lead to the occupation of other crystallographic positions by impurity atoms [12, 13]. In turn, DFT calculations of the free energy $\Delta G(x)$ (Gibbs thermodynamic potential) and mixing enthalpy ΔH_{mix} showed the energetic feasibility of the existence of semiconductor solid solutions $Lu_{1-x}Zr_x$NiSb and $Lu_{1-x}Sc_x$NiSb in the concentration interval $x = 0 \div 0.10$. At higher concentrations, the decomposition of the solid solution occurs.

The peculiarity of doping p-LuNiSb with the Zr dopant impurity (Zr has more d-electrons than Lu) is the metallization of electrical conductivity at the lowest concentration of Zr. The authors of work [12] associated the rearrangement of the electronic structure of $Lu_{1-x}Zr_x$NiSb with structural changes. Thus, replacing Lu atoms with Zr atoms or occupying the last vacancies in position $4a$ generates structural defects of the donor nature, and the corresponding donor states appear in the band gap ϵ_g. In the case of the substitution of Lu atoms for Sc in the $4a$ site in $Lu_{1-x}Sc_x$NiSb, defects of the neutral nature are generated (Lu and Sc atoms belong to the same group of the Periodic Table) [13]. When vacancies in position $4a$ are occupied by Sc atoms, defects of the acceptor nature and the corresponding acceptor states disappear, and defects of the donor nature and the corresponding donor states are generated. However, at all concentrations of $Lu_{1-x}Sc_x$NiSb, holes are the main charge carriers, and the Fermi level ϵ_F lies near the edge of the valence band ϵ_V. Thus, the number of generated donors is not enough to change the conductivity type of the semiconductor.

In this context, the case where V atoms ($3d^3 4s^2$) are introduced into the p-LuNiSb structure by replacing Lu atoms ($5d^1 6s^2$) in the $4a$ position, which should generate structural defects of the donor nature (V has more d-electrons than Lu). Since the atomic radius of V is much smaller than that of Lu ($r_{\text{Lu}} = 0.173$ nm) and close to the atomic radius of Ni ($r_{\text{Ni}} = 0.125$ nm), this may be a prerequisite for more complex changes in the crystal and electronic structures of $\text{Lu}_{1-x}\text{V}_x\text{NiSb}$ associated with a possible partial occupation of the $4c$ position by V atoms by filling vacancies and/or substituting Ni atoms. This is one of the subjects of the research presented below. Knowledge of the peculiarities of the dynamics of the crystal and electronic structures of $\text{Lu}_{1-x}\text{V}_x\text{NiSb}$ will allow the appropriate doping to fill vacancies and replace atoms of the base compound, by generating energy states that will meet the conditions for obtaining maximum values of the thermoelectric ZT-factor [2].

2. Experimental

Samples of the $\text{Lu}_{1-x}\text{V}_x\text{NiSb}$ ($x = 0 \div 0.10$) solid solution were synthesized by the arc-melting of a batch of appropriate amounts of Lu (99.9%), V (99.7%), Ni (99.99%), and Sb (99.999%) in the inert argon atmosphere followed by the homogenizing annealing at a temperature of 1073 K for 720 h. X-ray powder diffraction was performed on STOE STADI P (CuKα_1-radiation) and DRON-4.0 (FeKα-radiation) diffractometers. Lattice parameters were calculated using the Fullprof program [14]. The chemical and phase compositions of the samples were examined by energy dispersive X-ray spectroscopy (scanning electron microscope TESKAN VEGA 3 LMU). The DFT calculations were carried out with the Vienna Ab initio Simulation Package VASP v. 5.4.4 [15] with PAW-type potentials [16]. The Perdew–Burke–Enzerhoff exchange-correlation functional in the generalized gradient approximation (GGA) [17] with a $11 \times 11 \times 11$ Monkhorst–Pack k-point set [18] were used. The planewave cut-off was set to 400 eV in all calculations. For the crystal structures with mixed occupancies, the supercell approach was used. In this case, the symmetry of the lattics was reduced, and all unique atom distributions were generated using the combinatorial approach [19]. The lattice parameters for such structures were optimized by varying the lattice volume subsequently fitted by the universal equation of state [20]. The calculations of the elec-

tronic transport coefficients were carried out with the Exciting code [21] (FLAPW method) by solving the linearized Boltzmann equation in the constant relaxation time approximation [22–24]. The temperature and concentration dependences of the resistivity (ρ), thermopower coefficient (α) relative to copper, and magnetic susceptibility (χ) (Faraday method) were measured in the temperature interval $T = 80 \div 400$ K.

3. Results and Discussion

3.1. Investigation of thermodynamic and structural properties

The thermodynamic modeling of the hypothetical $\text{Lu}_{1-x}\text{V}_x\text{NiSb}$ solid solution showed positive values of the enthalpy of mixing in the whole concentration interval ($x = 0 \div 1.0$) (Fig. 2, a), which indicates that the Lu for V substitution is energetically unfavorable. However, the absolute values of the enthalpy of mixing are quite low. By applying the configurational entropy of mixing, it is possible to lower the free energy curve and to achieve a solubility of $x \approx 0.05$ at $T = 1000$ K. The study of the chemical and phase compositions of $\text{Lu}_{1-x}\text{V}_x\text{NiSb}$ samples, $x = 0 \div 0.10$, confirmed their overall composition, but, at the same time revealed the presense of a small amount of the LuNi$_3$ impurity concentrated between the grains of the main half-Heusler phase. Nevertheless, the EDX mapping showed that, up to 1 at.% ($x \approx 0.03$), Lu is substitited, indee, by V (Fig. 2, b) which is consistent with the thermodynamic modeling.

Based on the assumption that there is a continuous solid solution of $\text{Lu}_{1-x}\text{V}_x\text{NiSb}$, $x = 0 \div 1.0$, the change of the lattice parameter $a(x)$ for the ordered variant of the crystal structure was calculated by the PAW method (Fig. 3). In this case, all crystallographic positions are occupied by atoms corresponding to the MgAgAs structural type [1], and V atoms replace Lu atoms in position $4a$. Modeling the change in the period of the $\text{Lu}_{1-x}\text{V}_x\text{NiSb}$, $x = 0 \div 1.0$, (VASP [15]) shows a monotonous decrease of $a(x)$ (Fig. 3). The obtained result is expectable, since the substitution of large Lu atoms ($r_{\text{Lu}} = 0.173$ nm) with smaller V atoms ($r_{\text{V}} = 0.134$ nm) in position $4a$ will certainly lead to a decrease of the lattice parameter $a(x)$ of $\text{Lu}_{1-x}\text{V}_x\text{NiSb}$. At the same time, impurity donor states ϵ_D^V will be formed in the ϵ_g band gap of the $\text{Lu}_{1-x}\text{V}_x\text{NiSb}$ semiconductor (V has more d-electrons than Lu).
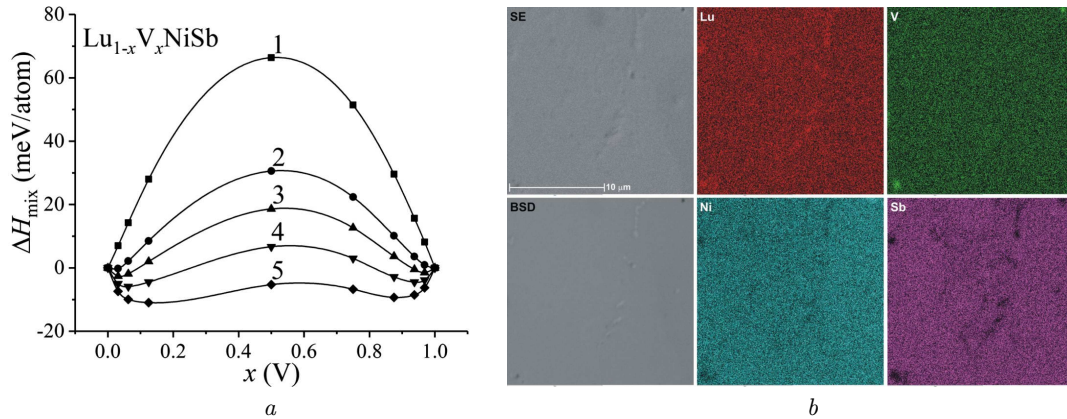
Fig. 2. Concentration dependences of the enthalpy of mixing $\Delta H_{\mathrm{mix}}(x)$ (*a*) and SEM pictures (SE/BSD) with the mapping of elements of a $Lu_{1-x}V_x NiSb$ sample ($x = 0.03$) (*b*). $T = 0$ K (*1*), $T = 600$ K (*2*), $T = 800$ K (*3*), $T = 1000$ K (*4*), $T = 1200$ K (*5*)

The powder XRD analysis showed that all powder patterns can be indexed in the MgAgAs-type structure and revealed the presence of a small amount of the impurity phase in all studied samples. Experimental values of the lattice parameters (Fig. 3, insert) of $Lu_{1-x}V_x NiSb$, $x = 0 \div 0.10$, deviate, at low concentrations, from the modeled ones and do not show a linear dependence. This may indicate that, in the crystal structure of $Lu_{1-x},V_x NiSb$ undergoes more complex changes than the elementary replacement of Lu atoms by V atoms. Based on the shape of the $a(x)$ dependence, one may speculate that the increase in the values of $a(x)$ at concentrations $x = 0 \div 0.03$ can occur, when V atoms occupy positions $4c$ of smaller Ni atoms ($r_{\mathrm{Ni}} = 0.125$ nm). At the same time, V atoms ($3d^3 4s^2$) can replace Ni atoms ($3d^8 4s^2$), by generating structural defects of the acceptor nature (V has fewer $3d$-electrons than Ni), and occupy available vacancies in the $4c$ position, by generating structural defects of the donor nature. At concentrations $x > 0.03$ (Fig. 3, insert), the behavior of the lattice parameter is obviously related to the predominant occupation of crystallographic position $4a$ of Lu atoms by V atoms. However, when comparing the modeled and experimental absolute values and slopes of the $a(x)$ dependence, it is easy to notice that, in comparison to the modeled one, the experimental dependence just barely decreases, confirming a very small solubility of V in LuNiSb.

3.2. Investigation of magnetic properties

Experimental measurements of the magnetic susceptibility $\chi(x)$ of $Lu_{1-x}V_x NiSb$ samples at room tem-

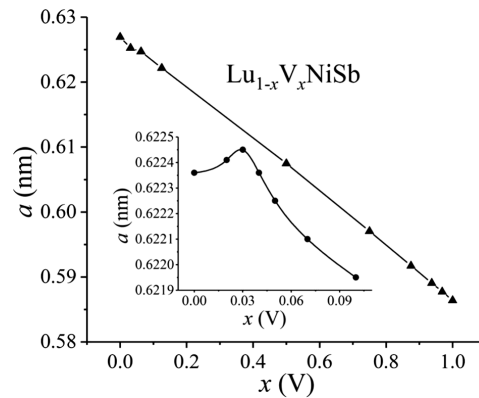**Fig. 3.** Modeling of the lattice parameter $a(x)$ of $Lu_{1-x}V_x NiSb$. Insert: experimental values of $a(x)$

perature (Fig. 4) showed that the semiconductor is a Pauli paramagnet with characteristically small values of the magnetic susceptibility ($\chi \sim 10^{-6}$ emu/g). It is known that, in Pauli paramagnets, the magnetic susceptibility is determined exclusively by the electron gas and is proportional to the density of electronic states at the Fermi level $g(\epsilon_{\mathrm{F}})$, and the results of measuring the magnetic susceptibility χ are a direct experimental method of establishing the fact of redistribution of the density of electronic states [9].

As is seen from Fig. 4, in the interval of concentrations $x = 0.01 \div 0.04$, the increase in the concentration of V atoms in the p-LuNiSb structure is accompanied by an increase in the magnetic susceptibility $\chi(x)$. However, at a concentration of $x \approx 0.04$, the dependence $\chi(x)$ of $Lu_{1-x}V_x NiSb$ passes through a maximum and, at $x > 0.04$, decreases to a concentra-

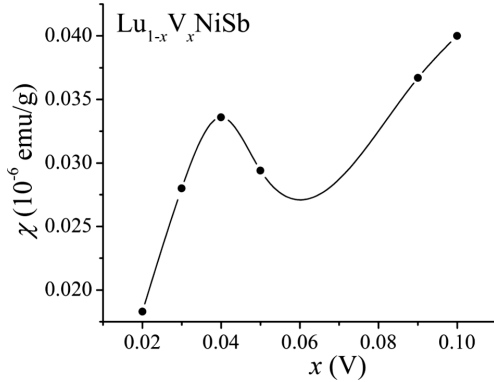**Fig. 4.** Concentration dependence of the magnetic susceptibility $\chi(x)$ of $Lu_{1-x}V_xNiSb$

tion of $x \approx 0.065$. Then, at $x > 0.07$, the magnetic susceptibility values increase again. Such N-like dependence of $\chi(x)$ for $Lu_{1-x}V_xNiSb$ is a reflection of structural changes that cause a redistribution of the density of electronic states at low V concentrations, where the solubility takes place, and the influence of the metallic impurity phase for higher V concentrations is observed.

3.3. Investigation of kinetic properties

The results of the DFT modeling and experimental studies of the temperature dependences of the resitivity $\rho(T,x)$ and thermopower coefficient $\alpha(T,x)$ of $Lu_{1-x}V_xNiSb$, $x = 0 \div 0.10$, are shown in Figs. 5–7. The calculated temperature dependences of the resistivity $\rho(T)$ of p-LuNiSb (FLAPW method [21–24]) coincides with that obtained earlier [12, 13] and shows a decrease in the resistivity at temperatures $T = 20 \div 50$ K (Fig. 5, a). This behavior of $\rho(T)$ is typical of semiconductors, when the number of free charge carriers increases due to their activation from the Fermi level ϵ_F to the conduction band. In the case of p-LuNiSb, holes are activated from the acceptor states ϵ_1^A into the valence band ϵ_V, and the main carriers are holes, which is indicated by the positive values of the thermopower coefficient $\alpha(T)$ (Fig. 6, a).

Doping p-LuNiSb with V atoms by substituting Lu atoms in the $4a$ position generates structural defects of the donor nature in the semiconductor $Lu_{1-x}V_xNiSb$, and the corresponding donor states ϵ_D^V appear in the ϵ_g band gap.

Modeling the resistivity $\rho(T,x)$ of $Lu_{1-x}V_xNiSb$ shows a rapid decrease in the temperature interval $T = 10 \div 35$ K. At temperatures $T > 35$ K, this

change is insignificant. At the same time, the values of the thermopower coefficient, for example, for the semiconductor $Lu_{0.99}V_{0.01}NiSb$ rapidly decrease and change their sign: $\alpha_{10 K} = 132.3 \mu V/K$ and $\alpha_{80 K} = -18.4 \mu V/K$ (Fig. 6). A change in the sign of the thermopower coefficient $\alpha(T,x)$ indicates a change in the type of conductivity, when electrons become the main charge carriers. The Fermi level ϵ_F is located in the conduction band ϵ_C, which ensures the metallic conductivity. At higher concentrations of V atoms, $x > 0.03$, at temperatures $T = 10 \div 400$ K, the sign of the thermopower coefficient $\alpha(T,x)$ remains negative, as does the metallic type of conductivity (Fig. 5, a). Obviously, at temperatures $T > 20$ K, there is a thermal ejection of electrons from donor states ϵ_D^V into the conduction band ϵ_C, which is accompanied by an increase in the concentration of free electrons. The Fermi level ϵ_F enters the conduction band ϵ_C: the insulator–metal conduction transition (Anderson transition [25]) takes place.

The experimental results for the resistivity $\rho(T,x)$ and the thermopower coefficient $\alpha(T,x)$ of the semiconductor $Lu_{1-x}V_xNiSb$, $x = 0 \div 0.10$ are presented in Fig. 7. We can see that, at all $Lu_{1-x}V_xNiSb$ concentrations, the temperature dependences of $\ln(\rho(1/T,x))$ and $\alpha(1/T,x)$ have high-temperature activation regions. This nature of a change in kinetic characteristics shows that the studied samples are doped and compensated semiconductors [26]. In addition, the presence of activation regions on the $\ln(\rho(1/T,x))$ dependences at high temperatures indicates the location of the Fermi level ϵ_F in the band gap ϵ_g, when charge carriers are activated into the conduction band. For samples with concentrations $x = 0- < 0.07$, the Fermi level ϵ_F lies closer to the valence band ϵ_V, as indicated by the positive values of the thermopower coefficient α at high temperatures (Fig. 7, b). However, at concentrations $x > 0.07$, the Fermi level ϵ_F is located near the edge of the conduction band ϵ_C, since the values of the thermopower coefficient α are negative at all temperatures.

The temperature dependences of $\ln(\rho(1/T,x))$ $Lu_{1-x}V_xNiSb$ (Fig. 7, a) can be described by formula (1) [26]:

$$\rho^{-1}(T) = \rho_1^{-1} \exp\left(-\frac{\varepsilon_1^\rho}{k_BT}\right) + \rho_3^{-1} \exp\left(-\frac{\varepsilon_3^\rho}{k_BT}\right), \quad (1)$$

where the first high-temperature term describes the activation of charge carriers $\epsilon_1^\rho(x)$ from the Fermi level
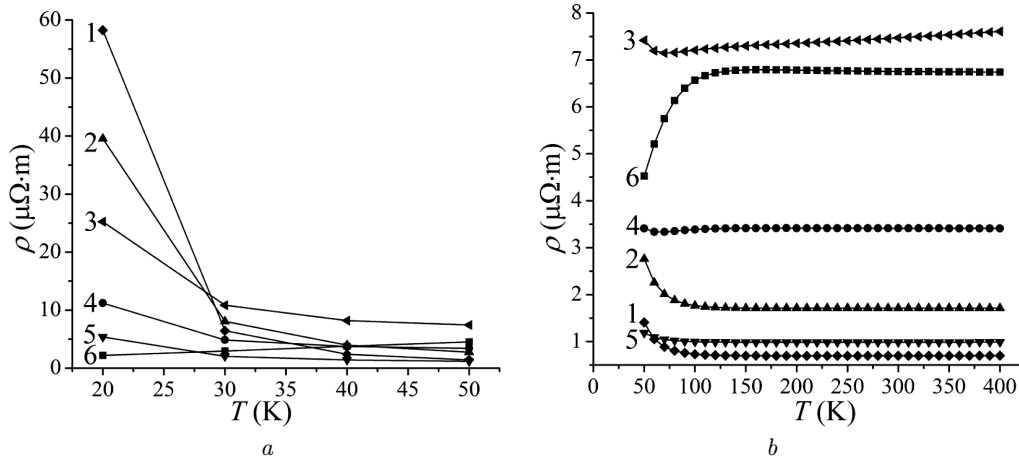
Fig. 5. DFT modeling of the temperature dependences of the resistivity $\rho(T, x)$ of $\text{Lu}_{1-x}\text{V}_x\text{NiSb}$ at low (*a*) and high (*b*) temperatures: $x = 0.10$ (*1*); $x = 0.04$ (*2*); $x = 0$ (*3*); $x = 0.02$ (*4*); $x = 0.07$ (*5*); $x = 0.01$ (*6*)
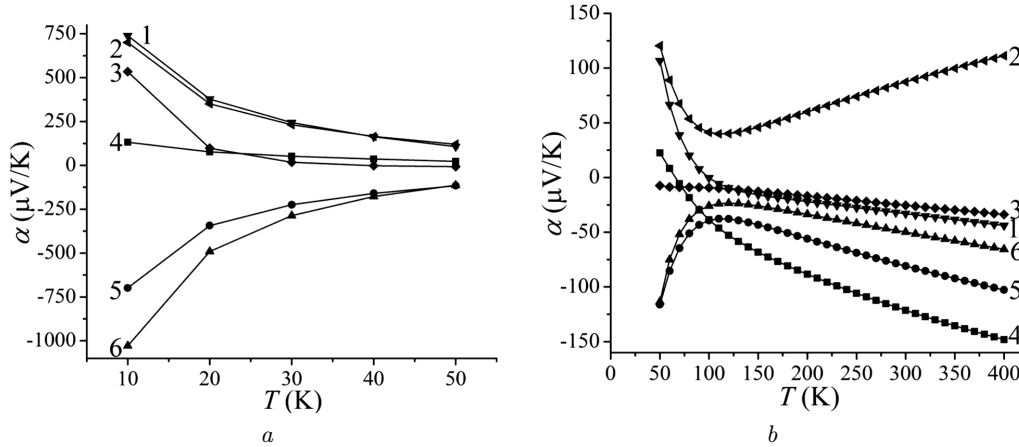

Fig. 6. DFT modeling of the temperature dependences of the thermopower coefficient $\alpha(T, x)$ of $\text{Lu}_{1-x}\text{V}_x\text{NiSb}$ at low (*a*) and high (*b*) temperatures: $x = 0.07$ (*1*); $x = 0$ (*2*); $x = 0.10$ (*3*); $x = 0.01$ (*4*); $x = 0.02$ (*5*); $x = 0.04$ (*6*)

ε_{F} into the valence band ε_V, and the low-temperature term describes the hopping conductivity $\epsilon_3^\rho(x)$ with energies close to the Fermi level ε_{F}.

The temperature dependence of the thermopower coefficient $\alpha(1/T, x)$ of $\text{Lu}_{1-x}\text{V}_x\text{NiSb}$ (Fig. 7, *b*) is described by formula (2) [23]:

$$\alpha = \frac{k_{\text{B}}}{e}\left(\frac{\varepsilon_V^\alpha}{k_{\text{B}}T} - \gamma + 1\right), \qquad (2)$$

where γ is a parameter that depends on the scattering mechanism. The values of the activation energies $\epsilon_1^\alpha(x)$ and $\epsilon_3^\alpha(x)$ were calculated from the high- and low-temperature activation regions of the $\alpha(1/T, x)$

dependence. Their values are proportional to the amplitude of the large-scale fluctuation of the continuous energy zones and the small-scale fluctuation of the compensated semiconductor [26].

As is seen from the temperature dependence of the resistivity $\ln(\rho(1/T, x))$ of *p*-LuNiSb in Fig. 7, *a*, there are the activation regions at high and low temperatures. The existence of the hopping ϵ_3^ρ-conductivity mechanism indicates the presence of a significant number of ionized acceptors in *p*-LuNiSb, which ensures carrier jumps to localized states in a vicinity of the Fermi energy ϵ_{F}. After all, in the structure of the *p*-LuNiSb semiconductor, there are vacancies in
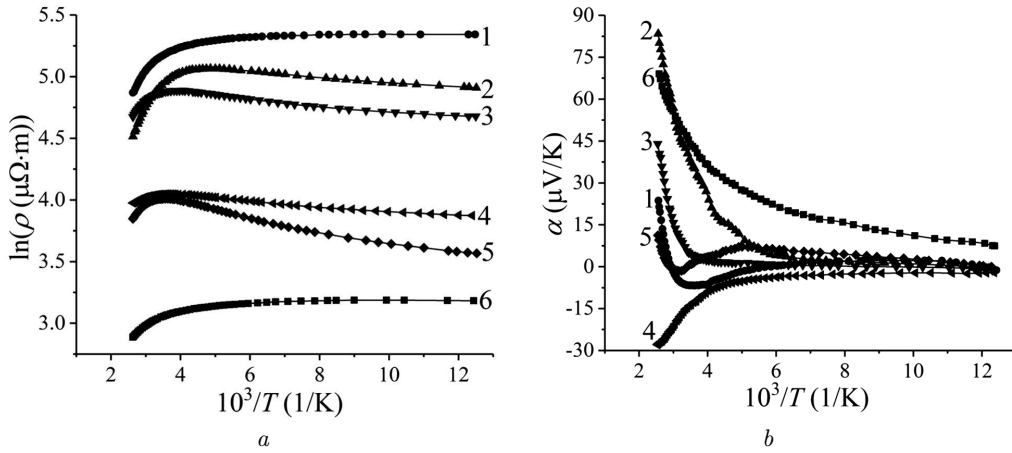
Fig. 7. Temperature dependences of the resistivity $\ln(\rho(1/T, x))$ (a) and thermopower coefficient $\alpha(1/T, x)$ (b) of $Lu_{1-x}V_xNiSb$: $x = 0.01$ (1); $x = 0.03$ (2); $x = 0.05$ (3); $x = 0.07$ (4); $x = 0.10$ (5); $x = 0$ (6)

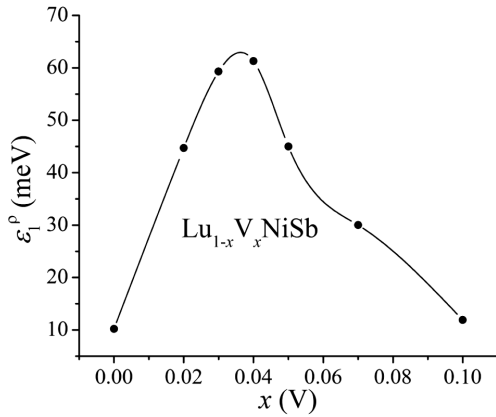**Fig. 8.** Change in values of activation energies $\epsilon_1^\rho(x)$ of $Lu_{1-x}V_xNiSb$

the positions of atoms $4a$ and $4c$ [7], which generates acceptor states ϵ_1^A in the band gap ϵ_g, and the Fermi level ϵ_F is located at a distance of ~ 10.2 meV from the edge of the valence band ϵ_V (Fig. 8).

For all other samples of $Lu_{1-x}V_xNiSb$, $x > 0$, there are no low-temperature activation areas and a mechanism of hopping ϵ_3^ρ-conductivity on the temperature dependences of the resistivity $\ln(\rho(1/T, x))$. An increase in the resistivity ρ at low temperatures in samples of $Lu_{1-x}V_xNiSb$, $x > 0$, indicates the metallization of conductivity, which, in the compensated semiconductors, is a sign of the proximity of impurity states that fix the Fermi level ϵ_F and the edge of the conduction band [26]. In the case of doped semiconductors $Lu_{1-x}V_xNiSb$, $x = 0.01- \leq 0.07$, this facili-

tates the ionization of acceptor states and the appearance of valence band holes ϵ_V. There is an overlap of the wave functions of the impurity states near the Fermi energy ϵ_F with the states of the valence band ϵ_V, forming a "tail" of the band, which leads to the metallization of conductivity.

From the results of experimental studies of the crystal structure, in particular, changes in the values of the unit cell period $a(x)$ (Fig. 3, insert), it was assumed that the generation of acceptor states ϵ_A^2 in a semiconductor is possible as a result of the partial replacement of Ni atoms $(3d^84s^2)$ by V atoms $(3d^34s^2)$ (V has fewer $3d$-electrons than Ni). The results of electrokinetic studies show the correctness of this assumption, since, in the experiment, we observed a change in the type of main charge carriers, which is mainly determined by the sign of the thermopower coefficient $\alpha(T, x)$ of $Lu_{1-x}V_xNiSb$.

The growth of the dependence of the thermopower coefficient $\alpha(1/T, x)$ in the interval $T = 80\div190$ K shows that, even at low temperatures, donors are generated in $Lu_{0.93}V_{0.07}NiSb$. The presence of a maximum in the dependence of $\alpha(1/T, x)$ at the temperature $T \approx 190$ K indicates that the rate of increase in the concentration of donors is greater than the rate of increase in the concentration of acceptors. The depletion of the acceptor band ϵ_A^1, generated by vacancies in the p-LuNiSb semiconductor structure, occurs. This leads to a change in the sign of the thermopower coefficient $\alpha(1/T, x)$ at the temperature $T \approx 294$ K. In turn, an increase in the nega-
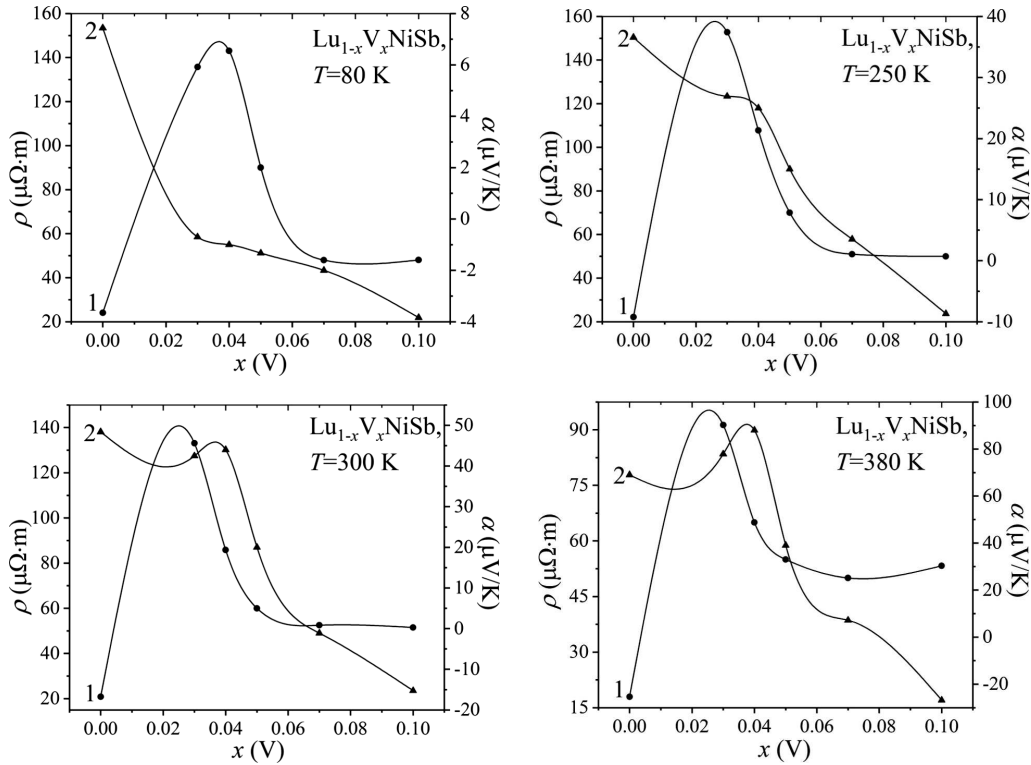
Fig. 9. Resistivity $\rho(x, T)$ and the thermoelectric coefficient $\alpha(x, T)$ of $Lu_{1-x}V_xNiSb$ at different concentrations and temperatures

tive values of the thermopower coefficient at temperatures $T = 294 \div 316$ K is the evidence of a change in the type of conductivity, when electrons become the main carriers of a semiconductor.

In $Lu_{0.99}V_{0.01}NiSb$, the depth of the Fermi level ϵ_F is ~ 23 meV. With increasing the concentration of V atoms, it increases to ~ 45 meV for $Lu_{0.98}V_{0.02}NiSb$ and ~ 59 meV for $Lu_{0.97}V_{0.03}NiSb$ (Fig. 8). Since, in the concentration interval $x = 0 \div 0.03$, the values of the activation energy of holes from the acceptor states ϵ_A^2 to the edge of the valence band ϵ_V increase almost linearly, this allows us to determine the drift speed of the Fermi level ϵ_F from the valence band ϵ_V: $\Delta \epsilon_F / \Delta x \approx 16$ meV/%V.

Similar conclusions can be reached by analyzing the concentration dependences of the resistivity $\rho(x, T)$ and the thermopower coefficient $\alpha(x, T)$ of $Lu_{1-x}V_xNiSb$ at different temperatures (Fig. 9). Thus, an increase in the resistivity $\rho(x, T)$ at concentrations $x = 0 \div 0.03$ in a p-type semiconductor is possible, only if the concentration of free holes decreases, which can happen, only if donors ap-

pear in the semiconductor, which compensate acceptor states by capturing holes. At the same time, there is an increase in the degree of compensation of the semiconductor $Lu_{1-x}V_xNiSb$. The nature of a change in the resistivity $\rho(x, T)$ and the thermoelectric coefficient $\alpha(x, T)$ of $Lu_{1-x}V_xNiSb$ in the interval of concentrations $x = 0 \div 0.03$ at different temperatures are consistent with the conclusion based on structural studies and clarify them. The analysis of changes in the lattice parameter $a(x)$ of $Lu_{1-x}V_xNiSb$ at concentrations $x = 0 \div 0.03$ showed that the growth can be caused by the partial occupation of the $4c$ position of Ni atoms by V atoms. The behavior of the thermoelectric coefficient $\alpha(x, T)$ of $Lu_{1-x}V_xNiSb$ for $x = 0 \div 0.03$ shows that the concentration of acceptors present in the semiconductor still exceeds the concentration of generated donors.

At a higher concentration of V atoms ($x = 0.04$), an extremum appears on the dependence of the resistivity $\rho(x, T)$ (Fig. 9), which shifts to the region of lower concentrations of V with increasing the temperature. The appearance of an extremum

on the dependence of $\rho(x,T)$ indicates changes in the ratio of ionized acceptors and donors present in $Lu_{1-x}V_xNiSb$. After all, an increase in the temperature simplifies the ionization of acceptors and donors. As a result, the concentration of free carriers increases.

The semiconductor $Lu_{0.93}V_{0.07}NiSb$ is doped and compensated and contains significant concentrations of electrons and holes. An increase in the concentration of V atoms ($x > 0.07$) is accompanied by a change in the type of main charge carriers from holes to electrons (Fig. 9). In turn, high concentrations of free electrons ensure the high conductivity of $Lu_{1-x}V_xNiSb$, and this has a slight effect on the change in the resistivity $\rho(x,T)$.

So, the experimental results of structural studies (Fig. 3, insert), magnetic susceptibility $\chi(x)$ (Fig. 4), resistivity $\rho(x,T)$, thermoelectric coefficient $\alpha(x,T)$ (Figs. 7 and 9), and the activation energy $\epsilon_1^\rho(x)$ (Fig. 8) of $Lu_{1-x}V_xNiSb$ revealed that V atoms can simultaneously occupy crystallographic positions $4a$ of Lu atoms and $4c$ of Ni atoms at $x = 0 \div 0.03$. At the same time, structural defects of the acceptor or donor nature are generated in the semiconductor, which leads to the appearance of the corresponding acceptor and donor states in the band gap ϵ_g. The concentration ratio of donor-acceptor states determines the position of the Fermi level ϵ_F and the mechanisms of electrical conductivity of $Lu_{1-x}V_xNiSb$.

4. Conclusions

A comprehensive study of the crystal and electronic structures, thermodynamic, kinetic, energy, and magnetic properties of the semiconductor $Lu_{1-x}V_xNiSb$ has shown the possibility for impurity V atoms to simultaneously occupy different crystallographic positions ($x = 0 \div 0.03$). At the same time, defects of the acceptor or donor nature are generated in the structure of the semiconductor $Lu_{1-x}V_xNiSb$, and the corresponding energy states appear in the band gap ϵ_g. The concentration ratio of donor-acceptor states determines the position of the Fermi level ϵ_F and the mechanisms of electrical conductivity of $Lu_{1-x}V_xNiSb$. The results of modeling the properties of the semiconductor are consistent with the data of experimental studies. Understanding the mechanism of energy state generation in the semiconductor $Lu_{1-x}V_xNiSb$ allows the modeling and produc-

tion of new thermoelectric materials with a high efficiency of converting the thermal energy into the electrical one.

1. K. Hartjes, W. Jeitschko. Crystal structure and magnetichyt56 properties of the lanthanoid nickel antimonides LnNiSb (Ln = La–Nd, Sm, Gd–Tm, Lu). *J. Alloys Compd.* **226**, 81 (1995).

2. L.I. Anatychuk. *Thermoelements and Thermoelectric Devices. Reference Book* (Naukova dumka, 1979) [in Russian].

3. I. Karla, J. Pierre, R.V. Skolozdra. Physical properties and giant magnetoresistance in RNiSb compounds. *J. Alloys Compd.* **265**, 42 (1998).

4. V.V. Romaka, L. Romaka, A. Horyn, P. Rogl, Yu. Stadnyk, N. Melnychenko, M. Orlovskyy, V. Krayovskyy. Peculiarities of thermoelectric half-Heusler phase formation in Gd–Ni–Sb and Lu–Ni–Sb ternary systems. *J. Solid State Chem.* **239**, 145 (2016).

5. K. Ciesielski, K. Synoradzki, I. Wolanska, P. Stachowiak, L. Kepinski, A. Jezowski, T. Tolinski, D. Kaczorowski. High-temperature power factor of half-Heusler phases RENiSb (RE = Sc, Dy, Ho, Er, Tm, Lu). *J. Alloys Compd.* **816**, 152596 (2020).

6. D. Gnida, K. Ciesielski, D. Kaczorowski. Origin of the negative temperature coefficient of resistivity in the half-Heusler antimonides LuNiSb and YPdSb. *Phys. Rev. B* **103**, 174206 (2021).

7. V.V. Romaka, L. Romaka, A. Horyn, Yu. Stadnyk. Experimental and theoretical investigation of the Y–Ni–Sb and Tm–Ni–Sb systems. *J. Alloys Compd.* **855**, 157334–12 (2021).

8. V.V. Romaka, Yu.V. Stadnyk, P.F. Rogl, L.P. Romaka, V.Y. Krayovskyy, A.Y. Horpenyuk, A.M. Horyn. Mechanism of Defect Formation $Zr_{1-x}V_xNiSn$ Thermoelectric Material. *Ukr. J. Phys.* **66**, 333 (2021).

9. V.A. Romaka, Yu.V. Stadnyk, V.Ya. Krayovskyy, L.P. Romaka, O.P. Guk, V.V. Romaka, M.M. Mykyychuk, A.M. Horyn. *The Latest Heat-Sensitive Materials and Temperature Transducers* (Lviv Polytechnic Publishing House, 2020) [in Ukrainian].

10. V.A. Romaka, Yu.V. Stadnyk, L.G. Akselrud, V.V. Romaka, D. Fruchart, P.F. Rogl, V.N. Davydov, Yu.K. Gorelenko. Mechanism of local amorphization of a heavily doped $Ti_{1-x}V_xCoSb$ intermetallic semiconductor. *Semiconductors* **42**, 753 (2008).

11. V.A. Romaka, P. Rogl, V.V. Romaka, D. Kaczorowski, Yu.V. Stadnyk, V.Ya. Krayovskyy, A.M. Horyn. Features

of conductivity mechanisms in heavily doped compensated $V_{1-x}Ti_xFeSb$ semiconductor. *Semiconductors* **50**, 860 (2016).

12. V.A. Romaka, Yu.V. Stadnyk, L.P. Romaka, V.Z. Pashkevych, V.V. Romaka, A.M. Horyn, P.Yu. Demchenko. Study of structural, thermodynamic, energy, kinetic and magnetic properties of thermoelectric material $Lu_{1-x}Zr_xNiSb$. *J. Thermoelectricity* **1**, 32 (2021).

13. V.V. Romaka, V.A. Romaka, Yu.V. Stadnyk, L.P. Romaka, P.Y. Demchenko, V.Z. Pashkevych, A.M. Horyn. Featutes of mechanisms of electrical conductivity in semiconductive solid solution $Lu_{1-x}Sc_xNiSb$. *Ukr. J. Phys.* **67**, 370 (2022).

14. T. Roisnel, J. Rodriguez-Carvajal. WinPLOTR: a windows tool for powder diffraction patterns analysis. *Mater. Sci. Forum, Proc. EPDIC7* **378–381**, 118 (2001).

15. G. Kresse, J. Hafner. Ab initio molecular dynamics for liquid metals. *Phys. Rev. B* **47**, 558 (1993).

16. G. Kresse, D. Joubert. From ultrasoft pseudopotentials to the projector augmented-wave method. *Phys. Rev. B* **59**, 1758 (1999).

17. J.P. Perdew, K. Burke, M. Ernzerhof. Generalized gradient approximation made simple. *Phys. Rev. Lett.* **77** (18), 3865–8 (1996).

18. H.J. Monkhorst, J.K. Pack. Special points for Brillouin-zone integrations. *Phys. Rev. B* **13**, 5188 (1976).

19. K. Okhotnikov, T. Charpentier, S. Cadars. Supercell program: a combinatorial structure-generation approach for the local-level modeling of atomic substitutions and partial occupancies in crystals. *J. Cheminform.* **8** (17), 1 (2016).

20. P. Vinet, J.H. Rose, J.S. Jr Ferrante. Universal features of the equation of state of solids. *J. Phys.: Codens. Matter.* **1**, 1941 (1989).

21. A. Gulans, S. Kontur, C. Meisenbichler, D. Nabok, P. Pavone, S. Rigamonti, S. Sagmeister, U. Werner, C. Draxl. Exciting – a full-potential all-electron package implementing density-functional theory and many-body perturbation theory. *J. Phys.: Condens Matter.* **26** 363202, 1 (2014).

22. B.R. Nag. *Electron Transport in Compound Semiconductors* (Springer Verlag, 1996).

23. G.D. Mahan and J.O. Sofo. The best thermoelectric. *Proc. Natl. Acad. Sci. USA* **93**, 7436 (1996).

24. T.J. Scheidemantel, C. Ambrosch-Draxl, T. Thonhauser, H.V. Badding, J.O. Sofo. Transport coefficients from first-principles calculations. *Phys. Rev. B* **68**, 125210 (2003).

25. N.F. Mott and E.A. Davis. *Electron Processes in Non-Crystalline Materials* (Clarendon Press, 1979).

26. B.I. Shklovskii, A.L. Efros. *Electronic Properties of Doped Semiconductors* (Springer-Verlag, 1984).

В.В. Ромака, В.А. Ромака,
Ю.В. Стадник, Л.П. Ромака, Й.О. Плевачук,
А.М. Горінь, М.З. Пашкевич, П.І. Гаранюк

ОСОБЛИВОСТІ
ГЕНЕРУВАННЯ ЕНЕРГЕТИЧНИХ СТАНІВ
У НАПІВПРОВІДНИКУ $Lu_{1-x}V_xNiSb$

Комплексне дослідження кристалічної та електронної структур, термодинамічних, кінетичних, енергетичних та магнітних властивостей напівпровідника $Lu_{1-x}V_xNiSb$, $x = 0$–0,10 встановило можливість домішкових атомів V одночасно займати різні кристалографічні позиції. При цьому у структурі $Lu_{1-x}V_xNiSb$ генеруються дефекти акцепторної та донорної природи, а в забороненій зоні ϵ_g з'являються відповідні енергетичні стани. Співвідношення концентрацій донорно-акцепторних станів визначає положення рівня Фермі ϵ_F та механізми електропровідності $Lu_{1-x}V_xNiSb$. Результати моделювання властивостей напівпровідника узгоджуються з даними експериментальних досліджень. Розуміння механізму генерування енергетичних станів у напівпровіднику у $Lu_{1-x}V_xNiSb$ дозволяє моделювати та отримувати нові термоелектричні матеріали з високою ефективністю перетворення теплової енергії в електричну.

К л ю ч о в і   с л о в а: рівень Фермі, електронна структура, електроопір, коефіцієнт термо-ерс.